The 2010 IEEE/RSJ International Conference on
Intelligent Robots and Systems
October 18-22, 2010, Taipei, Taiwan

Design and evaluation of a wearable haptic interface for large workspaces

Ingo Kossyk, Jonas Dörr and Konstantin Kondak

Abstract— **In this work we are evaluating the performance and design of a novel wearable haptic interface suitable for the appliance in large workspaces. We are investigating three main questions regarding the performance of the wearable haptic interface. The first question is whether stable and transparent presentation of contact with rigid surfaces on objects can be simulated with the wearable haptic interface. The second question is whether the performance of the haptic interface degrades when the user is able to walk around in the virtual environment while being tracked by a tracking system and using force feedback to navigate along rigid objects. The third question is whether the deflection of forces to the user's torso while operating the device disturbs the haptic interaction. In addition we are going to explain the mechanical construction of the wearable haptic interface and the dataflow of the virtual reality framework.**

I. INTRODUCTION

Haptic human computer interfaces have been regarded with an increasing interest by the research community over the last decade. These interfaces are an important performance factor for virtual reality systems in entertainment and for rapid prototyping tasks. As the workspace of a stationary haptic interface is limited a new field of research is regarding wearable designs. With these interfaces much larger workspaces can be exploited intuitionally compared to stationary devices. It needs to be emphasized though that former research on wearable haptic devices did not present experimental results of the actual haptic interaction while the user can walk around with the haptic interface and during which the exerted forces get deflected on the user's torso.

In this paper, we are going to present the results of haptic interaction of the user of a wearable haptic interface (WHI) while getting tracked in the workspace. In addition we are going to evaluate if the deflection of forces on the user's torso during haptic feedback is disturbing the grade of immersion. We present the mechanical design of a new wearable haptic interface and show the dataflow of the software framework. The device consists of a lightweight impedance controlled haptic feedback device based on an exoskeleton which can be carried like a backpack by the user. The user of this system is able to explore large-scale virtual environments with force feedback being presented to his hand and arm. The system's main fields of application are entertainment and virtual rapid prototyping.

This work was supported by the German Research Foundation (DFG).

Ingo Kossyk is with Faculty of Robotics, Technical University of Berlin, 10587 Berlin, Germany ikossyk@mailbox.tu-berlin.de

Jonas Dörr is with Faculty of Robotics, Technical University of Berlin, 10587 Berlin, Germany jdoerr@cs.tu-berlin.de

Konstantin Kondak is with department of robotics and mechatronics, DLR (German Aerospace Center), 82234 Wessling, Germany konstantin.kondak@dlr.de

II. RELATED WORKS

Proprioceptive haptic interfaces differ mainly in the mechanical approach and the control strategies. There are three main mechanical classes and two practical control strategies for the design of devices for haptic feedback: grounded, non-grounded and hybrid designs, following either impedance or admittance control schemes.

Grounded designs are fixed on a table or a special rig and can not be moved. This is why the workspace of a grounded device is rather limited. As the weight of the mechanics is not limited these devices can output high forces and provide inherent high mechanical stiffness. This is important for the stable and transparent presentation of rigid objects and hard contact surfaces. Examples for haptic interfaces in this class using an admittance control strategy for force feedback on the human upper limb can be found in [2]–[4].

Another class of devices follows a hybrid approach. The mechanics for force feedback are mounted on a mobile platform, thus combining good mechanical properties for haptic feedback with the access to large workspaces. Buss et al. have presented results in this field [6]. The inherent drawbacks of this approach are that the positioning of the mobile platform is afflicted with latency due to its inertia and actuation and that the used control strategies have to be rather robust in order to place the platform in an optimal way relative to the user's position. Wrong positioning leads to errors in the presentation of forces [7], [12].

Completely non-grounded devices must be supported by the user's body. The user carries the device around and is able to access an arbitrarily large workspace. Because of weight and ergonomics most non-grounded designs lack the properties which are inherent for grounded devices. The force output is limited due to the size and weight of the actuators as is the stiffness of the mechanical constructions. An example for a non-grounded wearable design is the portable exoskeleton actuated by admittance controlled pneumatic muscle actuators as presented by Tsagarakis et al. [5]. Because of inherent mechanical drawbacks of a wearable haptic device the application scenario of our work will be a multimodal compensated virtual reality system. Research has shown that it is feasible to exploit how the stimuli of the different modalities get merged into one immersive perception for the user [8], [9], [13]–[15].

Fig. 1. Current state of development of the WHI

TABLE I

WORKSPACE OF THE WHI AS GIVEN IN DEGREES BY THE JOINT ANGLES COMPARED TO THE MAXIMUM JOINT ANGLES OF THE WORKSPACE OF THE HUMAN UPPER LIMB

Joint	Human arm	WHI
Shoulder Abduction	134	107
Shoulder Adduction	48	60.5
Shoulder Flexion	188	147.5
Shoulder Extension	61	50
Elbow Flexion	142	108
Elbox Extension	–	–
Wrist Flexion	90	– (locked)
Wrist Extension	99	– (locked)
Wrist Adduction	27	360 (gimbal)
Wrist Abduction	47	360 (gimbal)
Forearm Supination	113	360 (gimbal)
Forearm Pronation	77	360 (gimbal)
Shoulder Medial Rotation	97	360 (gimbal)
Shoulder Lateral Rotation	34	360 (gimbal)

III. DESIGN OF THE WEARABLE HAPTIC INTERFACE

The WHI consists of a lightweight carbon based robotic arm mounted on a backpack with an overall of 5 degrees of freedom (3 actuated and 2 passive degrees of freedom). The torque for the lower joint is being transfered via a parallel four-bar linkage connected to a rotational degree of freedom at the mounting plate. The tooltip center point (TCP) is gimbal-mounted at the end of the lower link. In order to avoid singularities in the mechanics we locked one of the three rotational degrees of freedom of the gimbal. The remaining two degrees of freedom are not actuated, yet we attached optical encoders to them in order to track the orientation of the TCP. The gimbal between the TCP and the lower link improves ergonomics of the device a lot. The workspace of the WHI is designed to enable the user to freely move his arm in front of his torso when interacting with the virtual environment. A comparison of the angular limits in the joints of the human upper limb to the angular limits of the exosceleton is listed in Tab. I. These limits of the workspace have been proven as feasible as the user is free to rotate and move his body and thus translate and rotate the workspace of the device in world coordinates in order to get best access to the object he wants to interact with. We put a lot of care into the selection of the backpack as the tightness of the link between the user's torso and the haptic device's mounting point is crucial for stable force feedback and display of contact forces. The three active degrees of freedom are driven by brushed maxon RE40 motors via wire reductions similar to the gearing used in the DELTA [10] and PHANTOM [11] family of devices. The motors do not suffer from motor cogging due to their iron-free anchor. The specification of the motors is listed in Tab. III. In addition to that the rotor inertia is very low making the motor the optimal choice for an impedance controlled haptic interface. The transmission incorporates low friction and a high backdriveability. The transmission ratio is 1:20 for the two vertical axis and 1:15 for the horizontal axis. The motors are driven by copley digital servo controllers mounted on top of the mounting plate which is fixed just above shoulder height of the backpack. For the determination of the pose of the WHI we use optical encoders connected to the axis of the motors. The resolution of the used encoders is 4096 ticks per revolution. Magnetic sensors in the gearing wheels of the WHI are used to calibrate the sensor data and sense the initial pose of the WHI.

TABLE II

PRELIMINARY PARAMETERS OF THE WEARABLE HAPTIC INTERFACE

Parameter	Value
max. continnuos force	25 N (all axis)
max. peak force	40 N (all axis)
horizontal Span	1500 mm
vertical Span	1600 mm
Workspace Volume (stationary)	500 mm^3
Weight	13.5 Kg

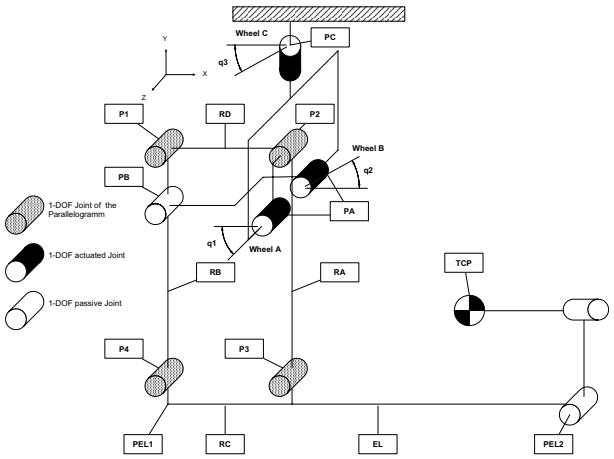

Fig. 2. Kinematic model of the WHI's mechanics

In Fig. 1 we depict the current state of development of the WHI. The end-effector is exchangeable in order to provide a flexible way to transfer the force between the user's hand

TABLE III
CHARACTERISTICS OF THE USED MAXON MOTORS RE40

Motor Specification	Value
Nominal voltage	48 V
Stall Current	41.4 A
Stall torque	2500 mNm
Rotor inertia	138 gcm^2
Weight	480 g

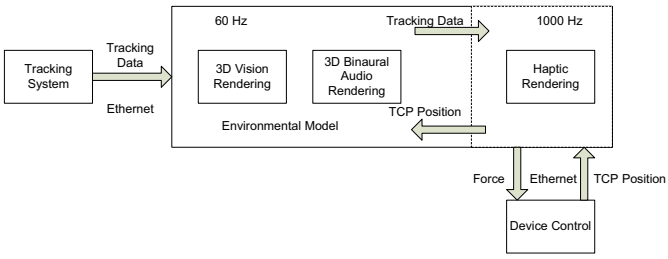

Fig. 3. Dataflow of the virtual reality system

and the haptic device. This makes the use of different end-effector tools like a joystick or a glove designed for special application scenarios possible. The whole device weighs approximately 13.5 kg and thus can be worn over a longer period of time without tiring the user ($>$ 1 hour). Fig. 2 shows the model used for the forward kinematic calculations. With this mechanical model of the device we are able to calculate the forward kinematics and torque that is required to be generated by the motors in order to output forces on either axis of the TCP in the device's local coordinate system.

IV. SYSTEM DESIGN PRINCIPLES

As listed in the previous section our approach for the WHI is based on lightweight and comparably cheap mechanics and is designed to give access to a large workspace. The fixture of the mechanics on the user's torso leads to a loss of stiffness when exerting contact forces which is a limiting factor for the grade of fidelity that can be experienced. Also high forces lead to a slight bending in the carbon exoskeleton arm worsening the stiffness of the WHI further. The effects of the drawbacks of these mechanical properties may be compensated by an adequate presentation of effects in other modalities. We want to describe the dataflow in the whole system for the sake of completeness and in order to describe how the haptic rendering is realized. The framework for rendering and control is designed as depicted in Fig. 3 and consists of three main components:

A. Tracking System

For tracking we use the Worldviz PPT-X optical tracking system in combination with two Intersense Inertiacube3. The system runs on a separate PC. The tracking data is made available via ethernet. We use the VRPN (Virtual Reality Peripheral Network Protocol) [16] to transfer the data to the core PC.

B. Core System

The core of the system consists of a multithreaded application. It is responsible for acquiring the tracking data from the tracking system with an update rate of 60Hz. It is subdivided into three modules each running associated processes and threads at different refresh rates.

- The visual core is processing the calculation of the 3D scene depending on the incoming positional data. It is updated at 60Hz for a smooth visual representation of the stereoscopic 3D environment. It also consists of the geometric and hierarchic information of the objects and the surroundings. For managing and rendering the scenegraph we use OSG (Open Scenegraph) [17].
- The audio core is synthesizing binaural audio queues depending on the geometry of the virtual room model and on the location and orientation of the user and sound sources in the virtual reality.
- The haptic core is rendering the appropriate forces depending on the geometric data of the scenegraph and the tracking data. There are constraints for a haptic system's update rate in order to generate stable forces during hard contacts and for the display of textures of arbitrary roughness. Because of this we chose an update rate of 1000Hz for the haptic thread to achieve stable and stiff contact forces similar to earlier works in the field e.g. [1]. The different update rates of acquisition of the tracking data and the haptic rendering thread introduces jitter during the display of contact forces. In order to minimize the effect of this jitter we apply a linear interpolation between successive updates of the translation and rotation of the haptic device. This adds a delay of 1/60th of a second to the system which can be neglected compared to the effect of jitter during hard contacts. As a framework for haptic rendering we use HAPI [18] and rely on the constraint based haptic rendering of contact forces between the TCP and virtual surfaces as presented by Ruspini et al. [19].

C. Control System

The calculated forces are sent via 100Mbit ethernet to the control module which is running on a separate embedded pc104-type PC mounted on the haptic device's backpack. For lowest possible latency the data is transfered via the UDP protocol. The control module is based on QNX RTOS in order to guarantee a refreshrate of 1000Hz and thus stable presentation of contact forces and time accurate acquisition of encoder data and button states. The module also includes the kinematic model of the haptic device in order to calculate the TCP position in local coordinates by solving the forward kinematics. The dynamics of the haptic device are compensated with a model based controller in order to minimize unwanted forces at the TCP caused by the mechanics inertia and mass. The PWM signals for the motor drivers are generated by a separate microcontroller. This ARM based microcontroller is also acquiring the encoder values via an I2C bus from five independent AVR Atmel microcontrollers.

Data transfer between the ARM microcontroller and the QNX RTOS is based on RS232 running at non-standard 1Mbit/sec transfer rate. To ensure the correct data transfer between the two units we use a CRC32 checksum.

V. DYNAMICS AND BASIC ALGORITHMS

For the control of the haptic device we derived the complete kinematic and dynamic model of the WHI. In this section we are going to show a simplified model of the geometric properties and distribution of masses of the WHI which we use for the calculation of the motor torques. We present a simplified dynamic model mostly due to the fact that velocities and accelerations in the mechanics during haptic interaction are low and the formulas of the complete model are slightly long. In the control loop we use the complete dynamic model. For the calculations of the torques we rely on the schematic model as shown in Fig. 2.

$$
\begin{aligned}
T_a = & -(G * L_{PA->P3} * M_{RA} * \cos q1 + G * L_{PA->P3} \\
& * M_{EL} * \cos q1 + G * L_{PA->P3} * M_{RB} * \cos q1 \\
& - L_{PA->P3} * F3 * \cos q1 - L_{PA->P3} * F1 * \sin q1 \\
& * \cos q3 - L_{PA->P3} * F2 * \sin q3 * \sin q1) \\
T_b = & -(L_{P3->PEL2} * F1 * \cos q3 * \cos q2 + L_{P3->PEL2} \\
& * F2 * \sin q3 * \cos q2 + G * M_{EL} * (L_{P4->PEL1} \\
& * \cos q2 + L_{P3->PEL2} * \sin q2) - L_{P4->PEL1} \\
& * F3 * \cos q2 - L_{P3->PEL2} * F3 * \sin q2 - G \\
& * L_{P1->P2} * M_{RB} * \sin q2 - L_{P4->PEL1} \\
& * F1 * \sin q2 * \cos q3 - L_{P4->PEL1} * F2 \\
& * \sin q3 * \sin q2) \\
T_c = & -(F1 * \sin q3 * (L_{P1->P2} * \sin q2 * L_{PA->P3} \\
& * \cos q1 - L_{P4->PEL1} * \cos q2 - (L_{P1->P2} \\
& + L_{P3->PEL2}) * \sin q2) - L_{PEL2->TCP} * F1 \\
& * \cos q3 - L_{PEL2->TCP} * F2 * \sin q3 - F2 * \cos q3 \\
& * (L_{P1->P2} * \sin q2 - L_{PA->P3} * \cos q1 \\
& - L_{P4->PEL1} * \cos q2 - (L_{P1->P2} \\
& + L_{P3->PEL2}) * \sin q2))
\end{aligned}
\tag{1}
$$

$G = 9.81 \frac{m}{s^2}$ is denoting the gravitational constant. T_a, T_b and T_c are the torques which have to be exerted at Wheel A, Wheel B and Wheel C. $F1$, $F2$ and $F3$ are the forces that get exerted at the TCP in X, Y and Z direction. We use the notation $L_{point1->point2}$ for the description of the links and M_{part} for the mass of a part of the mechanics. $q1$, $q2$ and $q3$ are the angles of wheel A, B and C. As this is a simplification of the more complex model in order to present it in this paper we also evaluated the overall error between the simplified and the exact model of the WHI. Compared to the exact model of the mechanics the simplification resulted in an error of up to 2 percent. This proves our simplification feasible. Haptic interaction is based on basic applied physics calculations. The two most important relationships in physics that are required to simulate most possible haptic effects are:

- The contact and coupling of the TCP with an arbitrary object can be described algorithmically by a spring-dampener model.
- The simulation of an object with a certain mass and inertia can be achieved by applying the physical model of an accelerated mass.

A. Spring-Dampener Model

When we want to model a coupling between the TCP and an object in the virtual world we have to apply a spring-dampener model for the calculation of the generated forces. This is also known as virtual coupling. In addition the contact of the TCP with a rigid object or surface can be modeled with this relation. As we are working with an impedance controlled haptic device the calculation of the appearing forces depends only on the position of the TCP in the virtual environment and properties of a virtual object. The spring-dampener model is defined as follows:

$$
\begin{aligned}
F_{TCP} &= F_S + F_D \\
F_S &= -k * \triangle p \\
F_D &= -c * v_{TCP}
\end{aligned}
\tag{2}
$$

Here k and c are constants describing the stiffness of the spring and the dampening (viscosity) factor respectively. $\triangle p$ is a scalar describing a penalty which occurs between the real TCP position and the object. This can be either the distance between the TCP and an object or the penetration depth of the TCP relative to an object's surface. With this relation we can model the virtual coupling or movement of an object with the TCP like a mass being connected to the TCP via a spring and a dampener.

B. Mass-acceleration

If we want to calculate forces due to inertia of an object's mass when coupled with the TCP we have to apply the physical model of an accelerated mass:

$$
F_{TCP} = m * a_{TCP} \tag{3}
$$

m is a constant describing the moving object's mass. Forces will only be exerted on the TCP if it is either being accelerated or decelerated while coupled to the mass.

VI. EXPERIMENTS AND RESULTS

In order to evaluate the performance of the system and the WHI we investigated three main questions. The first question is whether a stable and transparent presentation of contact with the rigid surfaces on objects can be achieved with the WHI. The second question is whether the performance of the haptic interface degrades when the user is able to walk around in the virtual environment while being tracked by the tracking system and using the force feedback to navigate along rigid objects. The third question is whether the deflection of forces to the user's torso while operating the device disturbs the haptic interaction.

We investigate the first and the second question by comparing the transparency of a contact with a stiff surface of the TCP in the stationary case (the WHI's workspace is not tracked and the virtual surface is located in the device's local coordinate system only) to the mobile case (the user is walking around carrying the device which is being tracked by the tracking system in order to recalibrate the workspace of the WHI in the world coordinate system). To evaluate the performance in the stationary case we setup a simple virtual wall in the coronal plane relative to the user with alternating stiffness and damping coefficients. The WHI was setup so that no tracking of the actual workspace in world-coordinates was implemented in order to evaluate the quality of a contact just in the local coordinates of the device. The user was instructed to move the TCP until he touches the wall. The virtual wall was put at 0.7 m at the X axis of the devices coordinate system. In all experiments the size of the sphere of the Ruspini renderer was set to 0.02 m. Fig.

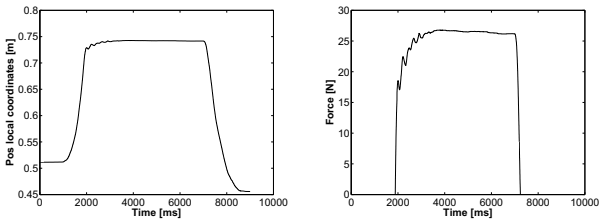

Fig. 4. Trajectory and rendered force during a contact of the TCP with a virtual wall in the coronal plane with stiffness k = 600 N/m and damping c = 40 $Nsec/m$

4 shows the trajectory of the TCP's position in the device's local coordinates compared to the force which was generated by the haptic renderer due to the contact with stiffness k = 600 N/m and dampening c = 40 $Nsec/m$. As shown in this figure, the penetration depth of the TCP relative to the virtual wall exceeded 0.72 m just by a few millimeters and the force graph shows stable behavior throughout the contact. The user reported the contact as being rigid and stable. Fig.

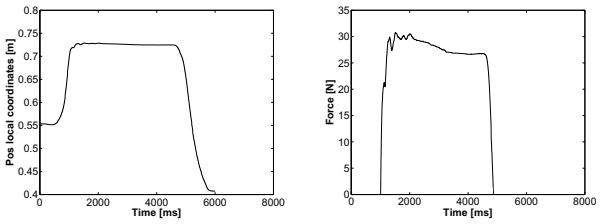

Fig. 5. Trajectory and rendered force during a contact of the TCP with a virtual wall in the coronal plane with stiffness k = 1000 N/m and damping c = 160 $Nsec/m$

5 shows the trajectory and rendered force of the device with a higher stiffness parameter k = 1000 N/m and dampening coefficient c = 160 $Nsec/m$. The position of the TCP did not exceed the constraint of 0.72 m, thus showing a stiff and stable contact. The graph of the force output shows a higher peak at the beginning when the contact is established. It still shows stable behavior of the WHI during the contact.

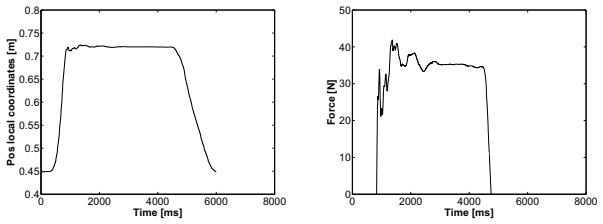

Fig. 6. Trajectory and rendered force during a contact of the TCP with a virtual wall in the coronal plane with stiffness k = 1600 N/m and damping c = 40 $Nsec/m$

Fig. 6 shows the behavior of the WHI during contact with high stiffness and low dampening coefficients. In this case the position trajectory and the rendered force are afflicted by oscillations which can be felt by the user specially at the point of time when contact is established. In this case the real force output at the devices TCP is clipped at 40 N by the motor drivers.

In the second experiment we investigated the performance of the WHI when its workspace in world-coordinates is getting tracked while the user walks around wearing the device. The importance of this topic needs to be emphasized as there are only a handful results of earlier works comparing the stationary / local performance of a wearable haptic device to the performance of the same device when it can be carried around by the user. To demonstrate the performance of the WHI in this scenario we recorded the trajectory of the TCP in world-coordinates. The user was instructed to intuitionally navigate along a virtual wall and a cylinder which were setup in the virtual environment. The user was wearing the

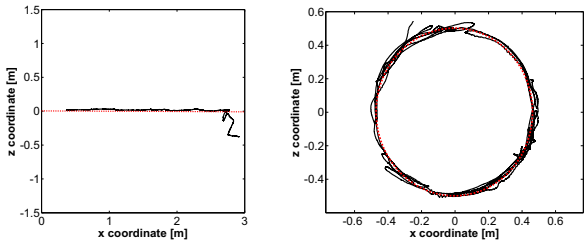

Fig. 7. Trajectory of the TCP during a trial in which the user explores a virtual wall along the x axis and a cylinder located at the origin of the world coordinate system with a radius of 0.5 m and stiffness k = 400 N/m and dampening c = 40 $Nsec/m$. The position and orientation of the user in world coordinates was used to recalibrate the translation and orientation of the workspace of the device. The red dotted line represents the boundaries of the objects

stereoscopic head-mounted display through which the virtual environment is displayed. This way the actual position of the user's hand in the real environment did not affect the sense of touch and immersion in the 3D-environment. The user was instructed to approach the wall with the haptic device and use his perception of touch to navigate along it. The stiffness and dampening was set to k = 400 N/m and c = 40

$Nsec/m$. The wall was located along the x-Axis of the world coordinate system. To compare the performance of the haptic device when used to explore more complex scenarios we performed the same experiment after exchanging the virtual wall with a virtual cylinder with a radius of 0.5 m located at the origin of the cartesian world coordinate frame. The results of both experiments are shown in Fig. 7. The user was able to navigate along both objects relying on his sense of touch. Of course the trajectory of the TCP does not follow the exact constraints of the objects at all times. This can be traced back to the fact that the user is actually carrying the device and walking around with it. The results show that the wearable design of the WHI is feasible for haptic interactions in large workspaces.

The third experiment examines the deflection of forces to the user's torso and whether this is worsening the perception of touching a virtual object. During interaction the generated forces at the TCP get deflected on the backpack and thus on the user's torso. It was not granted in the first place that this deflection does not disturb the grade of immersion. The results show that the exertion of forces on the torso and back of the user does not disturb the feeling of contact forces at the TCP. The user reported to actually perceive the contact with virtual objects as if he were to stand in the virtual environment, deflecting the forces on the object. This emphasizes the importance of the use of a high quality backpack to fix the haptic device on the user's torso. We reason that the large bearing area it provides and the mass of the user's torso compared to the forces during haptic interaction form a link that is stiff enough for a realistic presentation of interactions. For our work it is more than satisfactory as we are not aiming at a high force output but a realistic sensation of touch. The stiffness of the link between the backpack and the user's torso is crucial for a good transparency of the WHI.

VII. CONCLUSION AND FUTURE WORK

In this paper we have shown the principle designs of our system for human computer interaction in virtual realities. We have shown a wearable haptic interface's performance when used in large workspaces. A stable and transparent presentation of contact with the rigid surfaces on objects can be achieved with the WHI. Tracking of the WHI's position and orientation in order to recalibrate its workspace in world coordinates did not disturb the grade of the user's immersion when walking around in the virtual environment and using force feedback to navigate along rigid objects. The deflection of forces to the user's torso while operating the device did not disturb the sensation of touching virtual objects. The evaluation of these three topics also confirms that an exoskeleton for wearable haptics can perform appropriately in a virtual reality system with a large workspace. The exoskeleton showed excellent performance when delivering forces to the user's arm despite the fact that the linkage to the torso and the inherent mechanical properties worsened the stiffness of the overall system. The combination of stereoscopic vision with the wearable haptic device improved the sense of immersion. Future work will include the design of a high quality 3D demo application combining stereoscopic vision, 3D audio playback of contact sounds and haptic feedback. This will be used to evaluate the combination of the three modalities and from this evaluation conclusions will be drawn whether multimodal compensation is feasible to overcome the deficiencies of the WHI's mechanics.

VIII. ACKNOWLEDGMENTS

The authors want to thank the German Research Foundation for funding this research.

REFERENCES

[1] M. Minsky, Ming Ouh-young, O. Steele, F.O. Brooks, Jr.M. Behensky, Feeling and seeing, Issues in force display., *Computer Graphics*, vol.24, no.2, 1990, pp 235-243

[2] G.C. Burdea, Force and touch Feedback for Virtual Reality., *John Wiley & Sons Inc.*, 1996

[3] J. Burke, Exoskeleton Master Arm, Wrist and Effector Controller with Force Reflecting Telepresence., *Technical Report AL/CF-TR-1994-0146*, Odentics Inc., 1992, pp 104

[4] M. Ueberle, N. Mock, and M. Buss., ViSHaRD 10, a novel hyperredundant haptic interface., *Proceedings of the 12th International Symposium on Haptic Interfaces for Virtual Environment and Teleoperator Systems*, pp.58-65, March 2004.

[5] N. Tsagarakis, D.G. Caldwell and G.A. Medrano-Cerda, A 7 dof pneumatic Muscle Actuator (pMA) powered Exoskeleton, *Proceedings of the 1999 IEEE Internation Workshop on Robot and Human Interaction*, Pisa Italy, September 1999

[6] A. Peer, Y. Komoguchi and M. Buss, Towards a Mobile Haptic Interface for Bimanual Manipulations, *Proceedings of the 2007 IEEE/RSJ Internation Conference on Intelligent Robots and Systems*, San Diego, CA, USA, Oct 29 - Nov 2, 2007

[7] U. Unterhinninghofen, T. Schau and M. Buss, Control of a Mobile Haptic Interface, *Proceedings of the 2008 IEEE International Conference on Robotics and Automation*, Pasadena, CA, USA, May 19-23, 2008

[8] M.O. Ernst and H.H. Bülthoff, Merging the senses into a robust percept, *TRENDS in Cognitive Sciences*, Vol.8 No.4, April 2004

[9] Ernst, M. O. and M. S. Banks, Humans Integrate Visual and Haptic Information in a Statistically Optimal Fashion., *NATURE*, Vol.415 No.24 , January 2002

[10] R. Clavel, Une Nouvelle Structure de Manipulateur Parallle pour la Robotique Lgre., *APII*, vol.23, pp.501-519, 1989

[11] SensAble Technologies: http://www.sensable.com/

[12] A. Formaglio, and D. Prattichizzo, and F. Barbagli, and A. Giannitrapani, Dynamic Performance of Mobile Haptic Interfaces, *Robotics, IEEE Transactions on*, vol. 24, 2008, pp 559-575.

[13] Sulzer et al.,A Behavioral Adaptation Approach to Identifying Visual Dependence of Haptic Perception ,*WHC '07: Proceedings of the Second Joint EuroHaptics Conference and Symposium on Haptic Interfaces for Virtual Environment and Teleoperator Systems*, 2007, pp 3-8.

[14] Rock, Irvin and Victor, Jack, Vision and Touch: An Experimentally Created Conflict between the Two Senses, *Science*, vol. 143, 1964, pp 594-596.

[15] Treviranus, J., Adding haptics and sound to spatial curriculum,*Systems, Man, and Cybernetics, 2000 IEEE International Conference*, vol. 1, 2000, pp 588-592

[16] VRPN, Virtual Reality Peripheral Network, http://www.cs.unc.edu/Research/vrpn/

[17] OpensceneGraph, The OpenSceneGraph is an open source high performance 3D graphics toolkit. http://www.openscenegraph.org

[18] HAPI, HAPI is an C++ open source cross-platform haptics library., http://h3dapi.org/

[19] Ruspini, Diego C. and Kolarov, Krasimir and Khatib, Oussama, The haptic display of complex graphical environments., *SIGGRAPH '97: Proceedings of the 24th annual conference on Computer graphics and interactive techniques*,1997, pp 345-352